VOLUME 81 PAPER No. 775

PROCEEDINGS

AMERICAN SOCIETY
OF
CIVIL ENGINEERS

AUGUST, 1955

ANALOGIES USING NON-IDENTICAL EQUATIONS

by Robert Eugene Uhrig

ENGINEERING MECHANICS
DIVISION

{Discussion open until December 1, 1955}

Headquarters of the Society
33 W. 39th St.
New York 18, N. Y.

PRICE $0.50 PER COPY

This paper was published at 1745 S. State Street, Ann Arbor, Mich., by the American Society of Civil Engineers. Editorial and General Offices are at 33 West Thirty-ninth Street, New York 18, N. Y.

ANALOGIES USING NON-IDENTICAL EQUATIONS

Robert Eugene Uhrig[1]

ABSTRACT

A method of establishing analogies between two phenomena which do not have characteristic equations with identical forms has been presented. It differs from the usual procedure in that at least one of the equations relating the variables in the model to the corresponding quantities in the prototype is non-linear. This modified procedure is based upon a change in form of a characteristic equation when functional transformations are used.

An analog circuit was designed to predict the deflection of a column, and it was shown to give theoretical results which are identical with those in the literature. The use of a functional prediction equation made it possible to introduce resistance into the analog circuit even though the equation of a column does not contain a term with a first derivative.

An analog circuit for predicting the behavior of a simple vibrating system indicated that the use of a functional prediction equation liberalized the design conditions. It was also shown that a stable model could be used to predict an unstable condition.

A description of the design, construction and use of the electrical analog circuit to predict the deflections of a beam column for five different axial loads is presented. A photoformer was used in conjunction with a specially designed cathode follower amplifier having a low output impedance to supply an arbitrary voltage waveform to the analog circuit. The results of this investigation agree (within the limits imposed by the operation of the equipment) with the analytical solution of the beam column problem using the theory of elastic stability.

INTRODUCTION

The usual procedure for establishing an analogy is to match directly terms of equations having identical form or to use linear relationships between the variables of the equations. The purpose of this paper is to show that functional relationships can be used between the variables of the equations of the analogous systems to establish analogies between two phenomena which do not have characteristic equations with identical forms or to liberalize the analog design conditions.

The solution of many types of differential equations can be obtained by the substitution of one variable or quantity for another. This procedure often changes the differential equation into a form that is familiar and that can be solved by the use of standard methods. (An example of this procedure is the substitution of $z = \ln x$ to reduce a homogenous linear differential equation to a linear differential equation with constant coefficients.) The boundary

1. Iowa State College, Ames, Iowa.

conditions of the original problem must be transformed into terms of the new variables in order to evaluate the constants of integration. Then the transformations are used inversely to obtain the solution of the original problem. This general procedure can be adapted to aid in establishing analogies.

The method of establishing analogies used throughout this paper is the "Indirect Procedure" described by Murphy.[1] A simple example will illustrate this "Indirect Procedure" and how it can be modified to establish analogies between phenomena in which the characteristic equations are not identical.

Electrical Analog of a Column

The characteristic equation of an elastic column is

$$E I \frac{d^2 y}{d x^2} = - P y \tag{1}$$

which can be rewritten as

$$\frac{d^2 y}{d x^2} + \frac{P}{E I} y = 0 \tag{2}$$

where y, x, P, E, and I are deflection, distance from the origin, axial load, modulus of elasticity of the column material, and moment of inertia of the column cross-section respectively. An electrical model in which electrical charge (Q) varies with time (t) can be designed for the column. Prediction equations (sometimes called transformations or substitutions) are assumed to relate the variables of the two systems. Usually these prediction equations are assumed to be

$$y = n \; Q \quad \text{Dependent Variable} \tag{3}$$

$$x = n_1 \; t \quad \text{Independent Variable} \tag{4}$$

where n and n_1 are dimensional scales. If these transformations and their derivatives

$$\frac{d y}{d x} = \frac{n}{n_1} \frac{d Q}{d t} \tag{5}$$

$$\frac{d^2 y}{d x^2} = \frac{n}{n_1^2} \frac{d^2 Q}{d t^2} \tag{6}$$

are substituted into the characteristic equation (2) of the column, the resultant equation after simplification is

$$\frac{d^2Q}{dt^2} + \frac{Pn_1^2}{EI} Q = 0 \tag{7}$$

which has the same form as the original characteristic equation (2) but is expressed in terms of the new variables (Q) and (t).

The characteristic equation of the electrical circuit shown in Figure 1 after division by L is

$$\frac{d^2Q}{dt^2} + \frac{1}{LC} Q = 0 \tag{8}$$

where L and C are inductance and capacitance respectively. This equation (8) of the electrical system (the model) has the same form as equation (7), and equating of the coefficients of like terms in these two equations will give the design equation

$$\frac{Pn_1^2}{EI} = \frac{1}{LC} \tag{9}$$

However, if one or both of the prediction equations are functional rather than merely linear relationships, the resultant equation after substitution of the prediction equations and their derivatives will not have the same form as the original characteristic equation of the column. An example of a set of prediction equations in which one of the equations is functional and the other is linear is

$$y = n\, e^{\alpha t} Q \tag{10}$$

$$x = n_1\, t \tag{11}$$

where n, n_1, and α are dimensional constants. If the prediction equations (10) and (11) and their derivatives

$$\frac{dy}{dx} = \frac{n}{n_1} e^{\alpha t} \left(\frac{dQ}{dt} + \alpha Q \right) \tag{12}$$

$$\frac{d^2y}{dx^2} = \frac{n}{n_1^2} e^{\alpha t} \left(\frac{d^2Q}{dt^2} + 2\alpha \frac{dQ}{dt} + \alpha^2 Q \right) \tag{13}$$

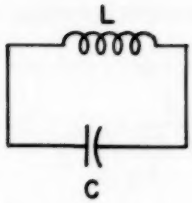

ELECTRICAL ANALOG CIRCUIT FOR A COLUMN

FIG. 1

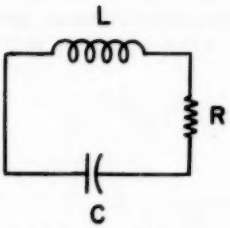

MODIFIED ELECTRICAL ANALOG CIRCUIT FOR A COLUMN

FIG. 2

are substituted into the characteristic equation (2) of the column, the resultant equation after simplification is

$$\frac{d^2Q}{dt^2} + 2\alpha \frac{dQ}{dt} + (\alpha^2 + \frac{Pn_1^2}{EI}) Q = 0 \qquad (14)$$

This transformed equation (14) can be matched term by term with the characteristic equation of an electrical circuit having a mathematically identical form, and the equating of coefficients will give the design equations for the electrical model.

The equation of the series electrical circuit shown in Figure 2 after division by L is

$$\frac{d^2Q}{dt^2} + \frac{R}{L} \frac{dQ}{dt} + \frac{1}{LC} Q = 0 \qquad (15)$$

which has the same form as the transformed equation (14). Matching of the coefficients of equations (14) and (15) gives the design equations

$$R/L = 2\alpha \qquad (16)$$

$$\frac{1}{LC} = \alpha^2 + \frac{Pn_1^2}{EI} \qquad (17)$$

Hence, an analogy has been established between two phenomena in which the characteristic equations (2) and (15) do not have the same form. (Throughout this paper, transformed or resultant equations such as equation (14) will not be considered as characteristic equations.)

The boundary conditions of the column must be transformed into boundary conditions of the electrical model by using the prediction equations, and these transformed boundary conditions must be satisfied in the electrical model if the analogy is to be valid. The boundary conditions for a column with knife edge supports on the ends are

$$x = 0, \; y = 0 \qquad (18)$$

$$x = \ell, \; y = 0 \qquad (19)$$

When the prediction equations (10) and (11) are applied to these boundary conditions, they become

$$t = 0, \; Q = 0 \qquad (20)$$

$$t = \ell/n_1 , \quad Q = 0 \tag{21}$$

Another boundary condition inherent in this analogy is that the solution of equation (15) must be of an oscillatory form, (i.e. damping in the model must not be over-critical.) The electrical circuit shown in Figure 2 can be built and used to determine the deflection of the column at any point by observing the charge (Q) in the electrical circuit at the proper time and then applying the prediction equations (10) and (11). Hence an analogy has been established between a mechanical system (the column) which has a characteristic equation with only the second derivative and the variable (y), and an electrical circuit having an equation with the second derivative, the first derivative, and the variable (Q).

Using a direct or linear prediction equation such as equation (3) instead of the functional prediction equation (10) was shown to give a circuit design with an inductance and a capacitance, but no resistance. Since any inductance inherently has some resistance, it is necessary to introduce resistance into the design of the analog circuit, or to compensate for this inherent resistance by using "negative resistances" or some type of feedback circuit.

The validity of this analogy can be shown theoretically by solving equation (14) assuming an oscillatory form of solution. This solution is

$$Q = e^{-\alpha t}\left[K_1 \operatorname{Sin}\left(\frac{P}{EI}\right)^{1/2} n_1 t + K_2 \operatorname{Cos}\left(\frac{P}{EI}\right)^{1/2} n_1 t\right] \tag{22}$$

where K_1 and K_2 are constants of integration. The transformed boundary condition (20) indicates that

$$K_2 = 0 \tag{23}$$

and substitution of (11), (22) and (23) into equation (10) will give

$$y = (n K_1) \operatorname{Sin}\left(\frac{P}{EI}\right)^{1/2} x \tag{24}$$

which is the equation of an elastic column where ($n K_1$) represents the maximum displacement of the column. If the boundary condition (21) is applied to equation (24), then

$$\operatorname{Sin}\left(\frac{P}{EI}\right)^{1/2} \ell = 0 \tag{25}$$

and hence

$$\left(\frac{P}{EI}\right)^{1/2} \ell = n_2 \pi \tag{26}$$

where n_2 is any integer. If n_2 is assumed to be 1, equation (26) becomes

$$P = \frac{\pi^2 E I}{\ell^2} \tag{27}$$

which is the well known Euler equation for a column with knife edge supports.

Electrical Analog of a Mechanical Vibrating System

The prediction equations (10) and (11) can also be used to an advantage in establishing an electrical analog of a mechanical vibrating system. This example will show how the design conditions may be made more flexible by going from the steady state to the transient state in the model.

The equation of motion of the simple vibrating system shown in Figure 3 is

$$\frac{w}{g}\frac{d^2y}{dx^2} + c\frac{dy}{dx} + Ky = F \cos \omega x \tag{28}$$

where y, x, W, g, c, K, F and ω are displacement, time, weight of the vibrating body, acceleration of gravity, damping coefficient, spring constant, amplitude of the shaking force and angular frequency of the shaking force respectively. Substitution of prediction equations (10) and (11) and their derivatives (12) and (13) into equation (28) gives

$$\frac{d^2Q}{dt^2} + \left(2\alpha + \frac{gcn_1}{w}\right)\frac{dQ}{dt} + \left(\alpha^2 + \frac{gcn_1\alpha}{w} + \frac{Kn_1^2 g}{w}\right)Q = \frac{Fgn_1^2}{wn} e^{-\alpha t} \cos \omega n_1 t \tag{29}$$

after simplification.

Application of Kirchoff's voltage law to the circuit shown in Figure 4

$$\frac{d^2Q}{dt^2} + \frac{R}{L}\frac{dQ}{dt} + \frac{1}{LC}Q = \frac{\varepsilon}{L}\cos \beta t \tag{30}$$

Equations (29) and (30) can be matched term by term to obtain the design conditions

$$R/L = 2\alpha + \frac{gcn_1}{w} \tag{31}$$

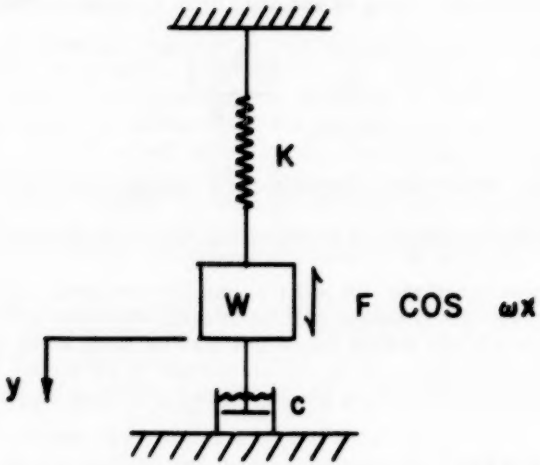

SCHEMATIC DIAGRAM OF A MECHANICAL VIBRATING SYSTEM

FIG. 3

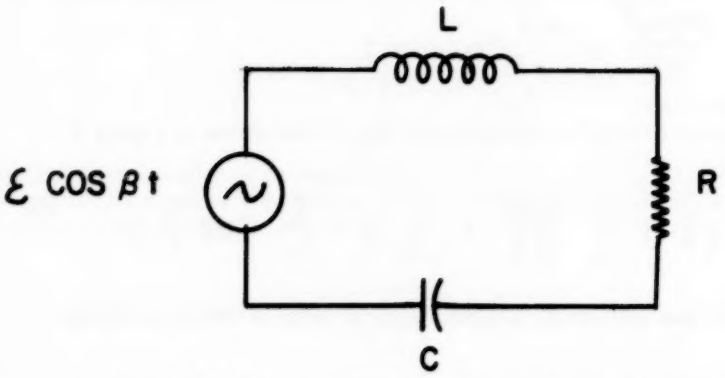

ELECTRICAL ANALOG CIRCUIT FOR THE MECHANICAL VIBRATING SYSTEM OF FIG. 3

FIG: 4

$$\frac{1}{LC} = \alpha^2 + \frac{g c n_1 \alpha}{w} + \frac{K g n_1^2}{w} \tag{32}$$

$$\mathcal{E}/L = \frac{F n_1^2 g}{n w} e^{-\alpha t} \tag{33}$$

$$\beta = n_1 \omega \tag{34}$$

Design equation (31) shows that the electrical model may have a large resistance even though the damping factor (c) in the mechanical vibrating system is quite small if a proper value of (α) is chosen. The principal limitation on this value of resistance is that the motion of the charge in the circuit must remain oscillatory. Design equation (34) permits the use of different frequencies in the prototype and the model, and equation (32) permits a wide selection of values for inductance and capacitance. Equation (33) means that the amplitude of the cosine voltage wave generated in the electrical circuit is decaying exponentially with model time (t), and hence the steady state condition in the electrical model is lost.

The analog circuit of Figure 4 can be built using a cosine wave voltage generator with some provision for decreasing the voltage amplitude exponentially, or by using an arbitrary function generator that can be adjusted to give any desired voltage wave shape. It is possible to start this exponentially decaying wave at properly timed intervals so that it appears as a steady state phenomenon when viewed on an oscilloscope.

Here again the analogy can be verified by solving the transformed equation (29), inversely applying the prediction equations (10) and (11), and then comparing the results with the known solution of the original system. The general solution of equation (29) is

$$Q = e^{-\alpha t}\left\{\frac{\frac{Fg}{wn}\left[\left(\frac{Kg}{w} - \omega^2\right)\operatorname{Cos}\ \omega n_1 t - \left(\frac{g\omega c}{w}\right)\operatorname{Sin}\ \omega n_1 t\right]}{\left(\frac{Kg}{w} - \omega^2\right)^2 + \left(\frac{g\omega c}{w}\right)^2}\right\}$$

$$+ e^{-\left(\alpha + \frac{g c n_1}{2w}\right)t}\left\{K_3 \operatorname{Cos}\left[\frac{g}{w}\left(K - \frac{g c^2}{4w}\right)\right]^{1/2} n_1 t \right. \tag{35}$$

$$\left. + K_4 \operatorname{Sin}\left[\frac{g}{w}\left(K - \frac{g c^2}{4w}\right)\right]^{1/2} n_1 t\right\}$$

where K_3 and K_4 are constants of integration. Substitution of (11) and (35) into prediction equation (10) gives after simplifications

$$y = \left\{ \frac{\frac{Fg}{w}\left[\left(\frac{Kg}{w} - \omega^2\right)\operatorname{Cos}\ \omega x - \left(\frac{g\omega c}{w}\right)\operatorname{Sin}\ \omega x\right]}{\left(\frac{Kg}{w} - \omega^2\right)^2 + \left(\frac{g\omega c}{w}\right)^2} \right\}$$

$$+ e^{-\frac{gc}{2w}x}\left\{K_3 \operatorname{Cos}\left[\frac{Kg}{w} - \left(\frac{gc}{2w}\right)^2\right]^{1/2} x \right. \tag{36}$$

$$\left. + K_4 \operatorname{Sin}\left[\frac{Kg}{w} - \left(\frac{gc}{2w}\right)^2\right]^{1/2} x \right\}$$

which agrees with the known results of the elementary theory of vibrations.

When there is no damping in the mechanical vibrating system and the shaking force has the same frequency as the natural frequency of the vibrating system, i.e.,

$$c = 0 \tag{37}$$

$$\omega = \omega_n = \left(\frac{Kg}{w}\right)^{1/2} \tag{38}$$

The solution of equation (29) for this special case of undamped resonance is

$$Q = e^{-\alpha t}\left[K_3 \operatorname{Cos}\ \omega_n\ n_1 t + K_4 \operatorname{Sin}\ \omega_n\ n_1 t \right. \tag{39}$$

$$\left. + \frac{F\omega_n n_1}{2Kn}\ t\ \operatorname{Sin}\ \omega_n\ n_1 t\right]$$

At first glance, it appears that (Q) becomes infinite with time because of the (t) in the last term of equation (39). However, the limit of $(t \cdot e^{-\alpha t})$ is zero as (t) approaches infinity, and the charge in the electrical circuit does not become infinite. However, substitution of (12) and (39) into prediction equation (11) gives

$$y = n K_3 \cos \omega_n x + n K_4 \sin \omega_n x + \frac{F \omega_n}{2K} x \sin \omega_n x \quad (40)$$

which indicates that the amplitude of vibration (y) does become infinite as time (x) approaches infinity for the special case of zero damping and vibration at the natural frequency. This also agrees with the known results of elementary vibration theory.

It is of interest to note that it is possible to predict an infinite amplitude of vibration in a mechanical system by using an electrical circuit which contains resistance and in which the electrical charge does not become infinite. Hence, a condition of instability can be predicted using a stable mode.

Electrical Analog of a Beam Column

The sketch of Figure 5 represents a beam column of length (ℓ) with axial load P and b lateral loads F_1, F_2, --- F_b at distances from the left end of a_1, a_2, --- a_b, respectively. The loads are applied in an upward direction so that the displacement of the beam column can be shown in a positive direction. The boundary conditions at the ends of the beam column are

$$x = 0, \; y = 0 \quad (41)$$

$$x = \ell, \; y = 0 \quad (42)$$

The equation of this beam column is

$$E I \frac{d^2 y}{dx^2} = M \quad (43)$$

where E, I, and M are modulus of elasticity of the beam column material, moment of inertia of the cross-section, and total bending moment in the beam column at any distance (x) from the origin, respectively. The equation for the bending moment, and hence the equation of the beam column, must be written in b + 1 parts, one for each portion of the beam column between the concentrated loads.

Figure 6 is a free body diagram of the left portion of the beam column shown in Figure 5 after it has been cut between loads F_m and F_{m+1}. For the interval

$$a_m \leq x \leq a_{m+1} \quad (44)$$

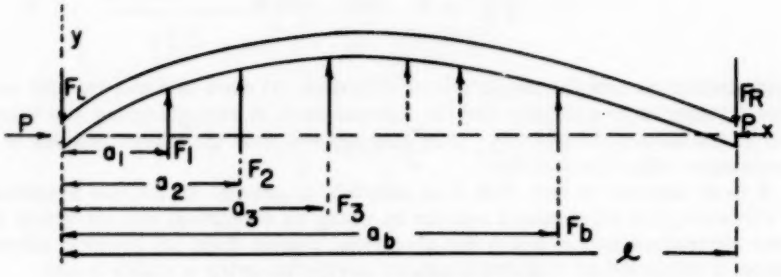

BEAM COLUMN WITH b LATERAL LOADS

FIG. 5

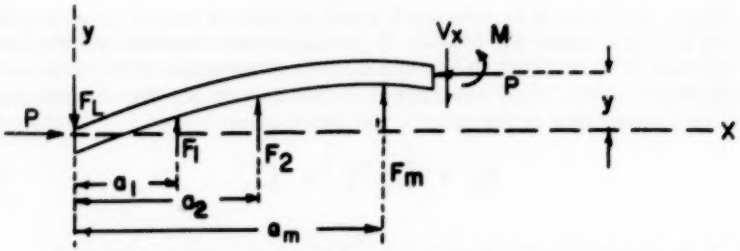

FREE BODY DIAGRAM OF A BEAM COLUMN CUT BETWEEN LOADS F_m AND F_{m+1}

FIG. 6

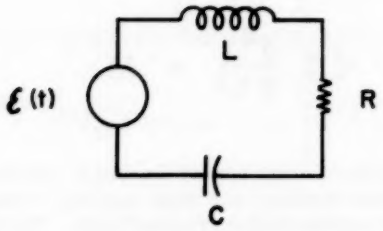

ANALOG CIRCUIT OF A BEAM COLUMN

FIG. 7

summation of moments to obtain the total bending moment M in the beam column at any distance x from the origin and substitution into equation (43) gives after simplification

$$\frac{d^2y}{dx^2} + \frac{P}{EI}\,y = \frac{M(x)}{EI} = -\frac{1}{EI}\left\{\left[\sum_{i=1}^{i=b} F_i\left(1-\frac{a_i}{\ell}\right)\right.\right. \tag{45}$$

$$\left.\left. + \sum_{i=1}^{i=m} F_i\right]x + \left[\sum_{i=1}^{i=m} F_i\, a_i\right]\right\}$$

where M(x) represents the equation for the moment due to the lateral loads alone for the interval (44).

If the prediction equations

$$y = n\, e^{\alpha t}\, Q \tag{46}$$

$$x = n_1\, t \tag{47}$$

and their derivatives

$$\frac{dy}{dx} = \frac{n}{n_1}\, e^{-\alpha t}\left[\frac{dQ}{dt} + \alpha\, Q\right] \tag{48}$$

$$\frac{d^2y}{dx^2} = \frac{n}{n_1 2}\, e^{-\alpha t}\left[\frac{d^2Q}{dt^2} + 2\alpha\frac{dQ}{dt} + \alpha^2 Q\right] \tag{49}$$

are the same as chosen previously for the column, substitution of (46) through (49) into equation (45) gives after simplification

$$\frac{d^2Q}{dt^2} + 2\alpha \frac{dQ}{dt} + \left(\alpha 2 + \frac{P n_1^2}{E I}\right) Q = e^{-\alpha t} \frac{n_1^2}{E I n} M(n_1 t)$$

$$= -e^{-\alpha t} \frac{n_1^2}{E I n} \left\{ \left[\sum_{\lambda=1}^{\lambda=b} F\lambda \left(1 - \frac{a\lambda}{\ell}\right) + \sum_{\lambda=1}^{\lambda=m} F\lambda \right] n_1 t \right. \tag{50}$$

$$\left. + \left[\sum_{\lambda=1}^{\lambda=m} F\lambda \, a\lambda \right] \right\}$$

where $M(n_1 t)$ represents the equation for the moment due to the lateral loads alone for the interval (44) transformed by the prediction equation (47).

The characteristic equation for the electrical circuit shown in Figure 7 which contains resistance, inductance, capacitance and an arbitrary voltage wave generator with output $\mathcal{E}(t)$ is

$$\frac{d^2Q}{dt^2} + \frac{R}{L} \frac{dQ}{dt} + \frac{1}{LC} Q = \frac{\mathcal{E}(t)}{L} \tag{51}$$

after division by L. Equations (50) and (51) can be matched term by term to give the following design conditions:

$$R/L = 2\alpha \tag{52}$$

$$\frac{1}{LC} = \alpha^2 + \frac{P n_1^2}{E I} \tag{53}$$

$$\frac{\mathcal{E}(t)}{L} = e^{-\alpha t} \frac{n_1^2}{E I n} M(n_1 t) \tag{54}$$

The right hand side of equation (50) represents a straight line for each interval (44) of the beam column, modified by an exponential decay factor $e^{-\alpha t}$. It can be easily seen by referring to equation (45), (47) and (50) that this series of straight lines is proportional to the moment diagram of the lateral loading on the beam column, transformed by the linear prediction equation (47), because the moment diagram is only a function of x. Therefore, the

shape of the output wave of the arbitrary voltage function generator used in this analog circuit must have the same shape (when viewed on an oscilloscope) as the moment diagram of the lateral loading, modified by the exponential decay factor $e^{-\alpha t}$.

The analog circuit consisted of four units, a resistance, a capacitance, an inductance, and an arbitrary function voltage generator. The resistance, capacitance, and inductance were commercial units, but the arbitrary function voltage generator was built. The type of arbitrary function voltage generator was built. The type of arbitrary function voltage generator chosen as the most practical from the standpoint of availability of equipment was a photoformer described by Sunstein.[2] The photoformer is essentially an electronic servo-system employing feedback to make the electron beam of a cathode ray oscilloscope follow a desired path as it is moved horizontally across the face of the tube by the sweep generator of the oscilloscope.

A Dumont 304-H cathode ray oscilloscope was the basic unit of this photoformer. A mask of the desired shape was made of black electrical tape and attached directly to the face of the cathode ray tube. A RCA 931-A photomultiplier tube was mounted in front of the cathode ray tube using the oscilloscope camera mounting bracket. The photomultiplier tube circuit is given in Figure 8. The output of the photomultiplier tube was connected to the direct coupled "Y" amplifier of the 304-H oscilloscope, and the output of the amplifier was connected to the vertical deflecting plates of the cathode ray tube. The feedback voltage applied to the vertical deflecting plates was of such polarity that increasing values of light intensity at the photomultiplier tube caused the spot to move downward. If the gain around the feedback loop is sufficient, the spot will be partially hidden behind the mask, and equilibrium will be maintained at this vertical position. Since the vertical deflection of the spot is proportional to the vertical deflecting voltage, the output is practically proportional to the height of the mask, for a given horizontal position. The horizontal position is controlled by the linear sweep generator in the oscilloscope.

The time to establish equilibrium and the exact height of the spot depends upon the total delay time around the feedback loop. This delay time includes the decay time of the phosphor screen plus the delay time of the photomultiplier tube and the amplifier. Of these, the decay time of the phosphor is the most important factor. A cathode ray tube having a persistence of P-11 emitting a blue light was used, because the P-11 surface has a short persistence and the 931-A photomultiplier tube is very sensitive to blue or blue-white light.

The output of this photoformer is a voltage wave of almost the same shape as the mask. The output impedance was very high and the power was quite low, and hence the photoformer could not be connected directly to the analog circuit. The direct coupled cathode follower amplifier shown in Figure 9 was used to match the impedances between the photoformer and the analog circuit and to amplify the power at the same time. This amplifier was developed specifically for use between the photoformer and the analog circuit employed in this experiment. Two 6L6 vacuum tubes operating in parallel amplify the power. The 6SN7 tube is used as an amplifier in the negative feedback circuit which decreases the output impedance to an extremely low value and also reduces the distortion of the waveform for large input signals. The VR-150 voltage regulator tube supplies a constant voltage of 150 volts for the plate of the 6SN7 tube. A Hewlett-Packard Model 710-A power supply was used as a plate voltage source for the cathode follower amplifier.

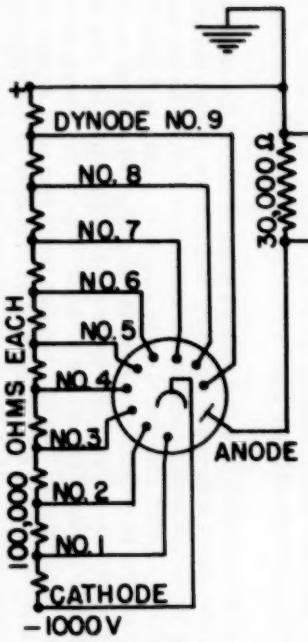

PHOTOMULTIPLIER TUBE CIRCUIT
FIG. 8

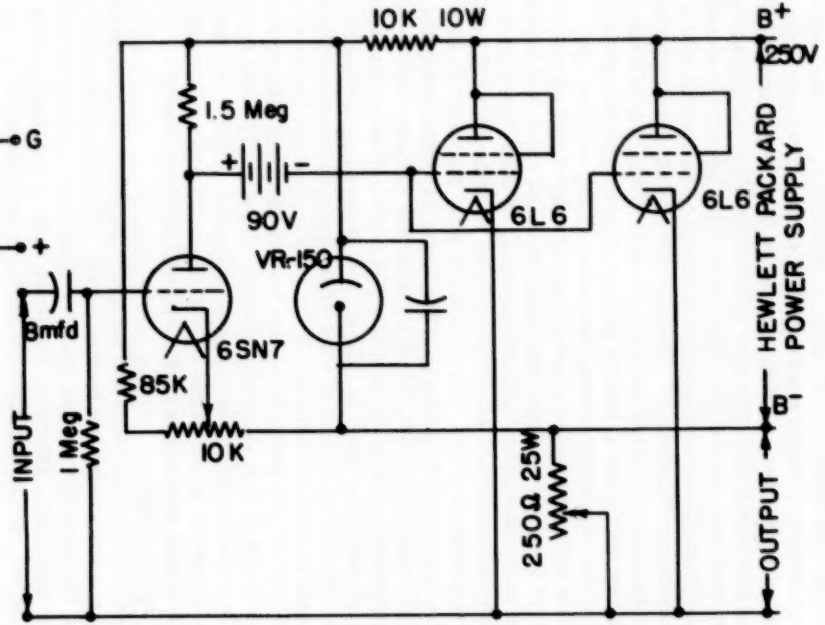

CIRCUIT DIAGRAM OF CATHODE FOLLOWER AMPLIFIER
FIG. 9

An audio frequency sine wave generator was used when adjusting the cathode bias of the cathode follower amplifier to give the largest undistorted output. With proper adjustment of both the cathode bias and the load resistor, it was possible to get an undistorted sine wave of 32 volts peak to peak and still not exceed the power output limitations of the Hewlett-Packard power supply.

A Dumont 303-AH oscilloscope used to measure the charge across the capacitance of the analog circuit provided a visual indication of the variation of the charge with time. The external synchronizer terminals of this oscilloscope were connected to the sweep signal output terminal of the oscilloscope used in the photoformer in order to synchronize the two oscilloscopes. A Dumont type 295 oscilloscope camera was mounted on the 303-AH oscilloscope to photograph the variation of voltage across the capacitance with time. The 303-AH oscilloscope has a built-in voltage calibrator which eliminated any voltage calibration difficulties.

The inductances consisted of two 63.7 millihenry coils that had been checked using an impedance bridge to determine both inductance and resistance. The capacitance across which the charge was measured consisted of a three-gang, one microfarad decade capacitor used with five oil filled capacitors which could be connected in series or parallel to give the desired value of capacitance. These capacitances were also calibrated on an impedance bridge. The resistance element included the effective resistance of the inductances, capacitances, and the output impedance of the cathode follower amplifier, as well as a 500 ohm variable resistor and other resistances which could be used to obtain the desired total resistance. Figure 10 is a block diagram of the entire analog system.

The beam column chosen for representation in the analog was a flat 3/16 inch by 1 inch by 60 inch aluminum alloy bar loaded as shown in Figure 11. The modulus of elasticity E of the aluminum alloy bar was assumed to be 10.5×10^6 psi, and the moment of inertia I of the cross section of the bar was calculated to be 7.32×10^{-4}, $in.^4$, giving a product EI of 40.1 $lb.\ ft.^2$. The shear and moment diagrams of the lateral loads on the beam column are shown in Figures 12 and 13.

The output of the photoformer has the shape of the moment diagram of the lateral loading multiplied by the exponential decay factor $e^{-\alpha t}$, and it is repeated in a cyclic manner as shown in Figure 14. This voltage waveform is fed to the analog circuit of Figure 7, and the voltage is measured across the capacitance to evaluate the electrical charge Q which is related to the displacement by prediction equation (46). Therefore, the voltage across the capacitance should have the general shape shown in Figure 15. However, it is not possible for the voltage across the condenser to change instantaneously as indicated by the sharp angle at point A in Figure 15, and the sharp angles would be rounded as shown in Figure 16 with inflection points at B and zero slopes at A. This could introduce serious errors into the results.

The method used to eliminate this difficulty and satisfy the boundary conditions was to use a mask having two waveforms, with the second waveform inverted and reversed (right to left) as shown in Figure 17. This eliminated the sharp change of applied voltage between cycles previously mentioned and the reintrant angles of the voltage waveform across the condenser as indicated in Figure 18. Since the photoformer gave better reproduction of the waveforms when the highest peaks were located at the ends of the mask, the mask was constructed from point F to point J in Figure 17 instead of from point D to point H.

At the right end of the beam column, the prediction equation (47) indicates that the τ is related to the beam column length by

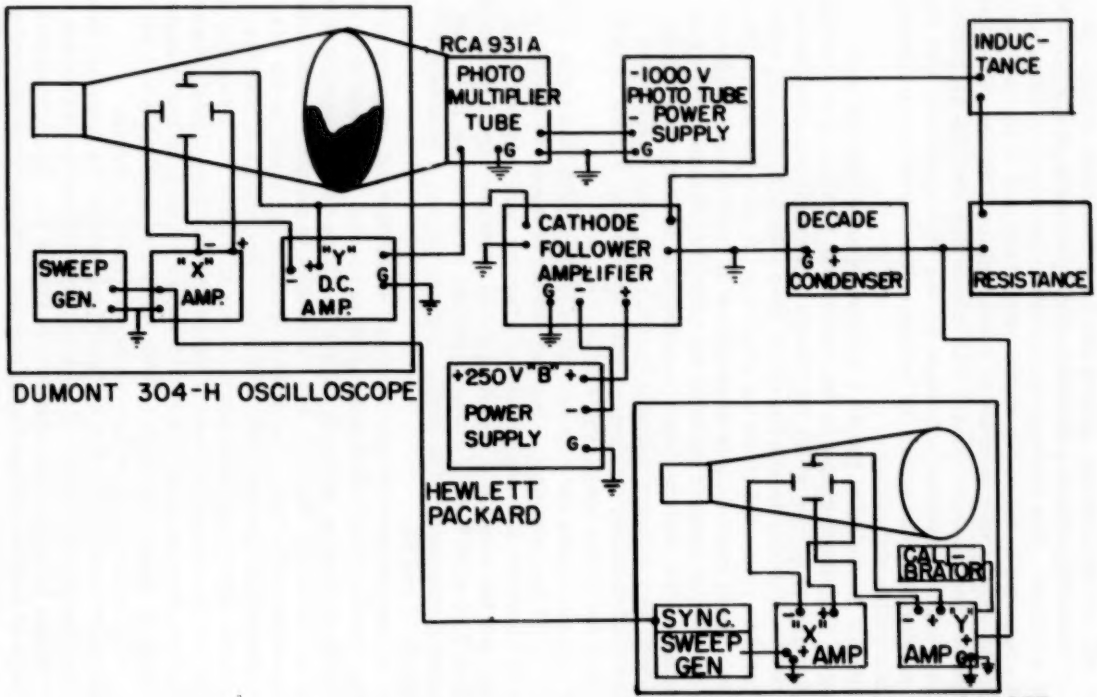

BLOCK DIAGRAM OF THE ANALOG SYSTEM
FIG. 10

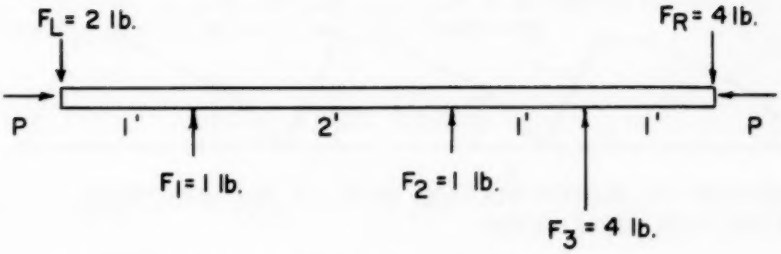

SKETCH OF LOADED BEAM COLUMN
FIG. 11

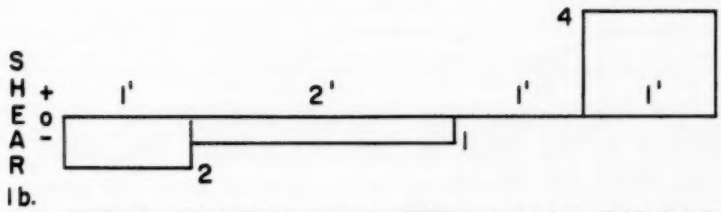

SHEAR DIAGRAM OF LATERAL LOADS FOR BEAM COLUMN SHOWN IN FIG. 11

FIG. 12

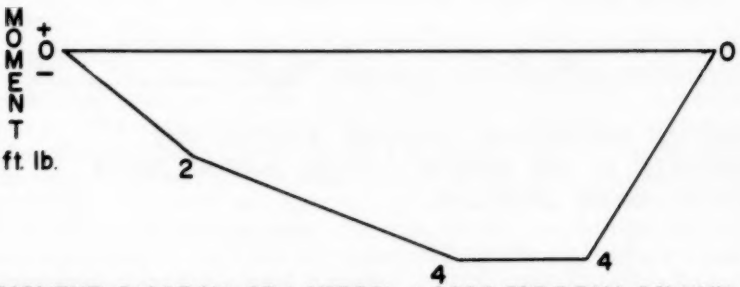

MOMENT DIAGRAM OF LATERAL LOADS FOR BEAM COLUMN SHOWN IN FIG. 11

FIG. 13

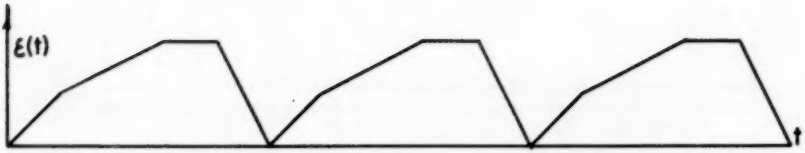

SKETCH OF OUTPUT VOLTAGE WAVE OF THE ARBITRARY FUNCTION GENERATOR

FIG. 14

SKETCH OF THE THEORETICAL VOLTAGE ACROSS THE CONDENSER IN THE ANALOG CIRCUIT HAVING THE INPUT VOLTAGE WAVE OF FIG. 14

FIG. 15

SKETCH OF THE ACTUAL VOLTAGE ACROSS THE CONDENSER IN THE ANALOG CIRCUIT HAVING INPUT VOLTAGE WAVE OF FIG. 14

FIG. 16

$$\ell = n_1 \tau \tag{55}$$

The time necessary for the cathode ray tube trace to make one sweep across the face of the tube (which is the reciprocal of sweep frequency) is equal to two τ periods, because the mask on the face of the cathode ray tube represents two complete cycles. Hence this relationship

$$\frac{1}{f} = 2\tau \tag{56}$$

can be substituted into equation (55) to give

$$f = \frac{n_1}{2\ell} \tag{57}$$

Another factor affecting the selection of a frequency is the frequency response of the photoformer and the cathode follower amplifier. The frequency response of the photoformer appeared to improve with frequency up to about 4000 cycles per second and then dropped quite rapidly. The frequency response of the cathode followed amplifier was good up to 10,000 cycles per second, but decreased to approximately one-half of its "flat range" value at 18,000 cycles per second. However, in amplifying voltage waveforms having sharp corners, it is necessary to accurately amplify at least the third (and preferably the fourth) harmonic of the fundamental frequency. Therefore a frequency of 3000 cycles per second was selected.

A change in the lateral loading of the beam column caused a change in the moment diagram, and hence required the construction of a new mask for the photoformer. However, a change in end load P can be represented in the analog circuit by a change in capacitance alone as indicated by design equation (53). Hence, it was decided to keep the lateral loading the same and vary the end loading.

A value of 1800/sec. was chosen for (α) because it allowed sufficient resistance in the analog circuit to take care of the inherent resistance of the inductances while introducing only a small damping factor in the electrical circuit. Two small wire wound inductors were connected in series to give a value of 0.1274 henry for inductance with a total resistance of 27.4 ohms. The output impedance of the cathode follower amplifier was measured to be 12.0 ohms. The total resistance needed in the analog circuit was calculated to be 459.0 ohms using equation (52). Therefore, the external resistance necessary to give this total resistance was 419.6 ohms, and a variable resistor was adjusted to give this value.

The value of (n) was calculated by equation (54) using the peak value of voltage and the moment corresponding to that peak voltage. Figure 19 is a large scale plot of the wave that is fed to the analog circuit. It can be easily seen that the upper and lower peak values of $M(x) \cdot e^{-\alpha t}$ (which is proportional to output voltage of the photoformer) are not equal. This is due to the factor $e^{-\alpha t}$ decreasing as t varies between 0 and and the peak moments of the two waves plotted do not occur at corresponding points. This face must

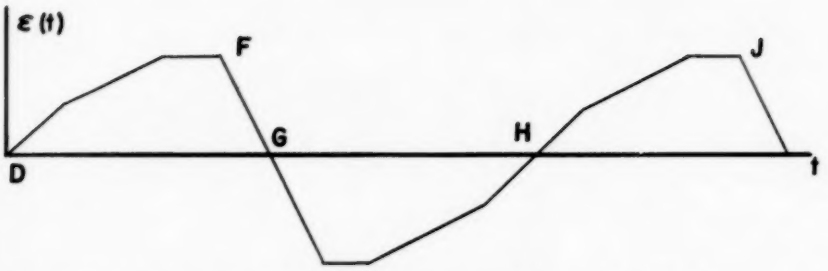

SKETCH OF THE OUTPUT VOLTAGE WAVE OF THE ARBITRARY FUNCTION GENERATOR WHEN EVERY OTHER WAVE IS INVERTED AND REVERSED.

FIG. 17

SKETCH OF THE THEORETICAL VOLTAGE ACROSS THE CAPACITANCE IN THE ANALOG CIRCUIT HAVING THE INPUT VOLTAGE WAVE OF FIG. 17.

FIG. 18

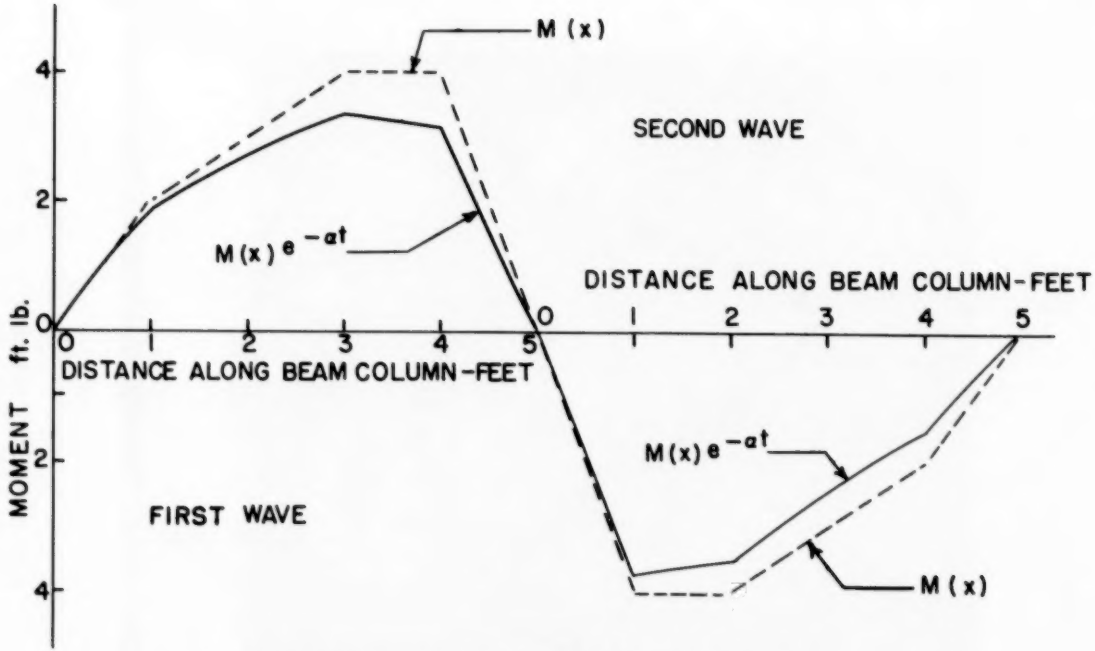

FIG. 19 PLOT OF MOMENT DIAGRAM AND OF ACTUAL WAVE FORM TO BE GENERATED BY PHOTOFORMER.

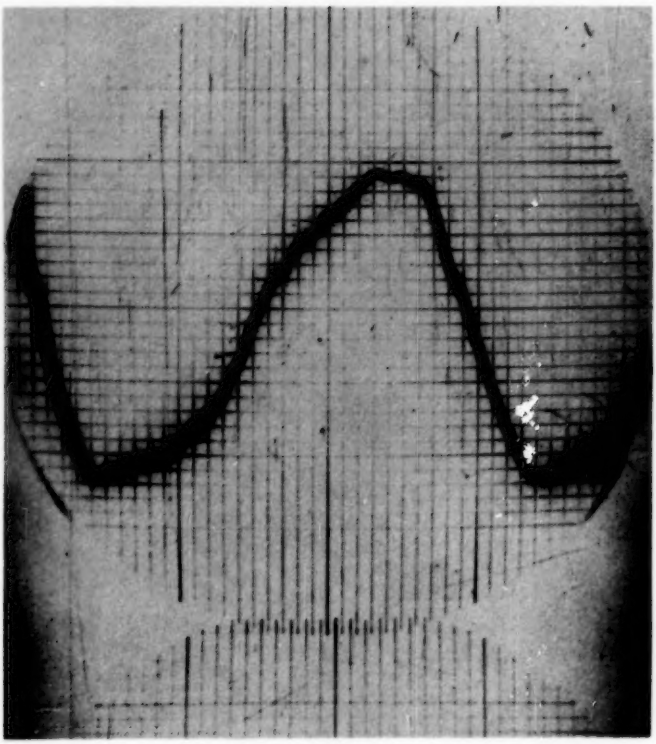

OUTPUT WAVE OF THE CATHODE FOLLOWER AMPLIFIER

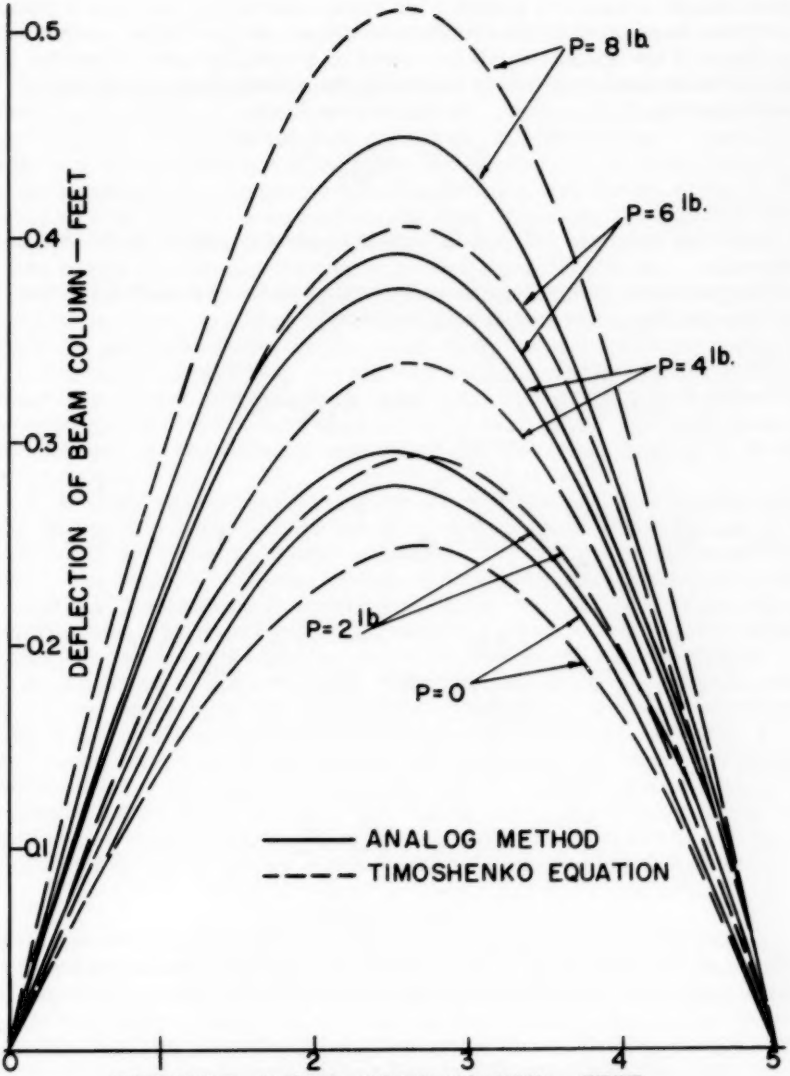

DEFLECTION CURVES OF BEAM COLUMN
FIG. 21

be taken into account when locating the reference axis on the output wave of the cathode follower shown in Figure 20.

The axial load P was varied in two-pound increments, up to 8 pounds, and equation (53) was used to determine the proper value of capacitance. The results of this experiment are the deflection curves of Figure 21 for the beam column loaded as shown in Figure 5 for axial loads of 0, 2, 4, 6 and 8 pounds.

Pictures were taken of the variation of voltage drop with time across the capacitance of the analog circuit as viewed on an oscilloscope. Since the charge Q in the analog circuit is related to the voltage drop across the capacitance by

$$Q = V_C \; C \tag{58}$$

the prediction equations (46) and (47) could be used to obtain the deflection curves.

The equation for the deflection of the beam column of Figure 5 between loads F_m and F_{m+1} is given by Timoshenko[3] to be

$$y = \frac{\sin KX}{P \sin K\ell} \sum_{i=m+1}^{i=b} F_i \sin K(\ell - a_i) - \frac{x}{P\ell} \sum_{i=m+1}^{i=b} F_i (\ell - a_i) + \frac{\sin K(\ell - x)}{P \sin K\ell} \sum_{i=1}^{i=m} F_i \sin K a_i - \frac{(\ell - x)}{P\ell} \sum_{i=1}^{i=m} F_i a_i \tag{59}$$

where

$$K = \left(\frac{P}{EI}\right)^{1/2} \tag{60}$$

Equation (59) was used to calculate values for the deflection curves given in Figure 21 for loads of 2, 4, 6, and 8 pounds. For zero axial load the deflection curve was calculated using the equation for the elastic curve of a beam.

The agreement between the experimental deflection curves for the beam column obtained from the analog circuit and the theoretical deflection curves obtained by the Timoshenko equation was fair. The experimental deflections were smaller than the theoretical deflections for larger values of axial load P and greater for small values of axial load. The error varied from about 3 per cent for an axial load of 2 pounds up to about 13 per cent for the 8 pound load.

The most obvious source of error in this experiment is the poor operation of the photoformer. It was found that the photomultiplier tube circuit loaded

the power supply so heavily that the negative 1000 volt direct voltage was decreased to approximately 350 volts. This dropped the acceleration voltage per dynode stage of the photomultiplier tube from 100 volts to approximately 35 volts which is not sufficient for proper operation. A larger power supply should solve this difficulty.

SUMMARY

A method of establishing analogies between two phenomena which do not have characteristic equations with identical forms and of liberalizing the analog design conditions has been presented. It differs from the usual procedure in that at least one of the equations relating the variables in the model to the corresponding quantities in the prototype is non-linear. This modified procedure is based upon a change in the form of a characteristic equation when the functional transformations are used.

An analog circuit was designed to predict the deflection of a column using a set of prediction equations containing one functional equation and one linear equation to establish the analogy even though the characteristic equations of these two phenomena were not identical. This use of a functional prediction equation made it possible to introduce resistance into the analog circuit even though the characteristic equation of a column does not contain a term with a first derivative. The results were shown to be identical with those given in the literature by theoretically solving the characteristic equation of the electrical circuit.

An analog circuit for predicting the behavior of a simple vibrating system was designed, showing that the use of a functional prediction equation made it possible to liberalize the design conditions. The theoretical solution showed that it was possible to predict an infinite deflection for an undamped system vibrating at the resonant frequency even though the analogous electrical system contained resistance and the electrical charge does not become infinite. Hence, a condition of instability can be predicted using a stable model.

An electrical analog circuit for a beam column was designed, using the procedure developed in this paper. The circuit was constructed and used to predict the deflections of a beam column for five different end loads. A photoformer was used in conjunction with a specially designed cathode follower amplifier having a low output impedance to supply an arbitrary voltage waveform to the analog circuit. The results of this investigation agree (within the limits imposed by the operation of the equipment) with the analytical solution of the beam column problem using the theory of elastic stability.

ACKNOWLEDGMENT

The author wishes to thank Dr. Glenn Murphy, Professor of Theoretical and Applied Mechanics and Head of the Department of Aeronautical Engineering at Iowa State College, Ames, Iowa, for the counsel and guidance he gave while directing this investigation.

REFERENCES

1. Murphy, Glenn. Similitude in Engineering, New York, Ronald Press Co., p, 237, 1950.

2. Sunstein, D. E. "Photoelectric Waveform Generator," Electronics, Vol 22 pp 100-104, 1949.

3. Timoshenko, S. Theory of Elastic Stability, New York, McGraw Hill Book Co., p 7, 1936.

PROCEEDINGS PAPERS

The technical papers published in the past year are presented below. Technical-division sponsorship is indicated by an abbreviation at the end of each Paper Number, the symbols referring to: Air Transport (AT), City Planning (CP), Construction (CO), Engineering Mechanics (EM), Highway (HW), Hydraulics (HY), Irrigation and Drainage (IR), Power (PO), Sanitary Engineering (SA), Soil Mechanics and Foundations (SM), Structural (ST), Surveying and Mapping (SU), and Waterways (WW) divisions. For titles and order coupons, refer to the appropriate issue of "Civil Engineering" or write for a cumulative price list.

VOLUME 80 (1954)

AUGUST: 466(HY), 467(HY), 468(ST), 469(ST), 470(ST), 471(SA), 472(SA), 473(SA), 474(SA), 475(SM), 476(SM), 477(SM), 478(SM)[c], 479(HY)[c], 480(ST)[c], 481(SA)[c], 482(HY), 483(HY).

SEPTEMBER: 484(ST), 485(ST), 486(ST), 487(CP)[c], 488(ST)[c], 489(HY), 490(HY), 491(HY)[c], 492(SA), 493(SA), 494(SA), 495(SA), 496(SA), 497(SA), 498(SA), 499(HW), 500(HW), 501(HW)[c], 502(WW), 503(WW), 504(WW)[c], 505(CO), 506(CO)[c], 507(CP), 508(CP), 509(CP), 510(CP), 511(CP).

OCTOBER: 512(SM), 513(SM), 514(SM), 515(SM), 516(SM), 517(PO), 518(SM)[c], 519(IR), 520(IR), 521(IR), 522(IR)[c], 523(AT)[c], 524(SU), 525(SU)[c], 526(EM), 527(EM), 528(EM), 529(EM), 530(EM)[c], 531(EM), 532(EM)[c], 533(PO).

NOVEMBER: 534(HY), 535(HY), 536(HY), 537(HY), 538(HY)[c], 539(ST), 540(ST), 541(ST), 542(ST), 543(ST), 544(ST), 545(SA), 546(SA), 547(SA), 548(SM), 549(SM), 550(SM), 551(SM), 552(SA), 553(SM)[c], 554(SA), 555(SA), 556(SA), 557(SA).

DECEMBER: 558(ST), 559(ST), 560(ST), 561(ST), 562(ST), 563(ST)[c], 564(HY), 565(HY), 566(HY), 567(HY), 568(HY)[c], 569(SM), 570(SM), 571(SM), 572(SM)[c], 573(SM)[c], 574(SU), 575(SU), 576(SU), 577(SU), 578(HY), 579(ST), 580(SU), 581(SU), 582(Index).

VOLUME 81 (1955)

JANUARY: 583(ST), 584(ST), 585(ST), 586(ST), 587(ST), 588(ST), 589(ST)[c], 590(SA), 591(SA), 592(SA), 593(SA), 594(SA), 595(SA)[c], 596(HW), 597(HW), 598(HW)[c], 599(CP), 600(CP), 601(CP), 602(CP), 603(CP), 604(EM), 605(EM), 606(EM)[c], 607(EM).

FEBRUARY: 608(WW), 609(WW), 610(WW), 611(WW), 612(WW), 613(WW), 614(WW), 615(WW), 616(WW), 617(IR), 618(IR), 619(IR), 620(IR), 621(IR)[c], 622(IR), 623(IR), 624(HY)[c], 625(HY), 626(HY), 627(HY), 628(HY), 629(HY), 630(HY), 631(HY), 632(CO), 633(CO).

MARCH: 634(PO), 635(PO), 636(PO), 637(PO), 638(PO), 639(PO), 640(PO), 641(PO)[c], 642(SA), 643(SA), 644(SA), 645(SA), 646(SA), 647(SA)[c], 648(ST), 649(ST), 650(ST), 651(ST), 652(ST), 653(ST), 654(ST)[c], 655(SA), 656(SM)[c], 657(SM)[c], 658(SM)[c].

APRIL: 659(ST), 660(ST), 661(ST)[c], 662(ST), 663(ST), 664(ST)[c], 665(HY)[c], 666(HY), 667(HY), 668(HY), 669(HY), 670(EM), 671(EM), 672(EM), 673(EM), 674(EM), 675(EM), 676(EM), 677(EM), 678(HY).

MAY: 679(ST), 680(ST), 681(ST), 682(ST)[c], 683(ST), 684(ST), 685(SA), 686(SA), 687(SA), 688(SA), 689(SA)[c], 690(EM), 691(EM), 692(EM), 693(EM), 694(EM), 695(EM), 696(PO), 697(PO), 698(SA), 699(PO)[c], 700(PO), 701(ST)[c].

JUNE: 702(HW), 703(HW), 704(HW)[c], 705(IR), 706(IR), 707(IR), 708(IR), 709(HY)[c], 710(CP), 711(CP), 712(CP), 713(CP)[c], 714(HY), 715(HY), 716(HY), 717(HY), 718(SM)[c], 719(HY)[c], 720(AT), 721(AT), 722(SU), 723(WW), 724(WW), 725(WW), 726(WW)[c], 727(WW), 728(IR), 729(IR), 730(SU)[c], 731(SU).

JULY: 732(ST), 733(ST), 734(ST), 735(ST), 736(ST), 737(PO), 738(PO), 739(PO), 740(PO), 741(PO), 742(PO), 743(HY), 744(HY), 745(HY), 746(HY), 747(HY), 748(HY)[c], 749(SA), 750(SA), 751(SA), 752(SA)[c], 753(SM), 754(SM), 755(SM), 756(SM), 757(SM), 758(CO)[c], 759(SM)[c], 760(WW)[c].

AUGUST: 761(BD), 762(ST), 763(ST), 764(ST), 765(ST)[c], 766(CP), 767(CP), 768(CP), 769(CP), 770(CP), 771(EM), 772(EM), 773(SA), 774(EM), 775(EM), 776(EM)[c], 777(AT), 778(AT), 779(SA), 780(SA), 781(SA), 782(SA)[c], 783(HW), 784(HW), 785(CP), 786(ST).

c. Discussion of several papers, grouped by Divisions.

AMERICAN SOCIETY OF CIVIL ENGINEERS

OFFICERS FOR 1955

PRESIDENT

WILLIAM ROY GLIDDEN

VICE-PRESIDENTS

Term expires October, 1955:
ENOCH R. NEEDLES
MASON G. LOCKWOOD

Term expires October, 1956:
FRANK L. WEAVER
LOUIS R. HOWSON

DIRECTORS

Term expires October, 1955:
CHARLES B. MOLINEAUX
MERCEL J. SHELTON
A. A. K. BOOTH
CARL G. PAULSEN
LLOYD D. KNAPP
GLENN W. HOLCOMB
FRANCIS M. DAWSON

Term expires October, 1956:
WILLIAM S. LaLONDE, JR.
OLIVER W. HARTWELL
THOMAS C. SHEDD
SAMUEL B. MORRIS
ERNEST W. CARLTON
RAYMOND F. DAWSON

Term expires October, 1957:
JEWELL M. GARRELTS
FREDERICK H. PAULSON
GEORGE S. RICHARDSON
DON M. CORBETT
GRAHAM P. WILLOUGHBY
LAWRENCE A. ELSENER

PAST-PRESIDENTS

Members of the Board

WALTER L. HUBER
DANIEL V. TERRELL

EXECUTIVE SECRETARY
WILLIAM H. WISELY

TREASURER
CHARLES E. TROUT

ASSISTANT SECRETARY
E. L. CHANDLER

ASSISTANT TREASURER
CARLTON S. PROCTOR

PROCEEDINGS OF THE SOCIETY

HAROLD T. LARSEN
Manager of Technical Publications

DEFOREST A. MATTESON, JR.
Editor of Technical Publications

PAUL A. PARISI
Assoc. Editor of Technical Publications

COMMITTEE ON PUBLICATIONS

SAMUEL B. MORRIS, *Chairman*

JEWELL M. GARRELTS, *Vice-Chairman*

GLENN W. HOLCOMB
OLIVER W. HARTWELL
ERNEST W. CARLTON
DON M. CORBETT